VİTANATUR
İLAÇ KOZMETİK AR-GE DAN. A.Ş.
Pharmaceutical & Cosmetic R&D Consulting Ltd.

+90-507 840 65 04
info@vitanaturtr.com

19.01.2026

Evaluation of Intestinal Permeability of Calcium Butyrate Using the SPIP Model

To the Relevant Authority,

This report has been prepared to evaluate the intestinal permeability profile of calcium butyrate (CAB) and the accompanying in vitro release/kinetic modeling findings using the Single-Pass Intestinal Perfusion (SPIP) approach.

In the study, the dissolution behavior of CAB under gastrointestinal conditions was investigated using the dialysis membrane method; the release data were interpreted with the zero-/first-order, Higuchi, Hixson–Crowell, and Korsmeyer–Peppas models. In the in situ SPIP experiments, phenol red and metoprolol were used as markers to verify membrane integrity and method performance; following net water flux corrections, effective permeability (Peff) and human predictions were calculated.

The methodology, calculations, and findings are presented in report format in the sections below.

Prof. Dr. Neslihan Üstündağ Okur

VİTANATUR
İLAÇ KOZMETİK BİTKİSEL
ÜRÜNLER ARGE DANIŞMANLIK A.Ş.
Kavacık Mah. Ekinciler Cad. A Blok Rektörlük
Medipol Üniversitesi No: 19/3 Beykoz İSTANBUL
Beykoz V.D.: V.K.N. 9251220772

Abbreviations

Calcium Butyrate: CAB

Metoprolol: MTP

Phenol Red: PR

Single-Pass Intestinal Perfusion: SPIP

+90-507 840 65 04
info@vitanaturtr.com

1. METHODS

1.1. Development of HPLC Method

The chromatographic separation was achieved on a Develosil column C18, 150 Å~ 3 mm, 4.6 µm particle size with isocratic elution. The mobile phase was composed of methanol: phosphate buffer (20 mM, pH 3.1) (43:57, v/v). 2.7 g of sodium dihydrogen phosphate and 420 µL of phosphoric acid were dissolved, then the mixture was sonicated for 10 minutes. The buffer solution and the other mobile phase component, methanol, were degassed before use and filtered. The injection volume was 20 µL, and the column oven temperature was set at 30 °C. The flow rate of the method was chosen 1 mL/min. The UV detector was set at 206 nm wavelength obtained maximum absorbance from MTP, PR and CAB[1]. Agilent 1200 series HPLC device was used.

1.2. *In Vitro* Release Studies

The release study was performed dialysis bag (Spectra/Por Dialysis membrane/molecular weight of 12–14 kDa) method. Gastric (pH 1.2) media were used as the release medium. 100 mg CAB was placed in the dialysis bag and closed with closures. The filled dialysis bags were immersed in 100 mL of gastric media providing sink conditions and mixed at 37 ± 0.5 °C with a magnetic stirrer at 100 rpm. The membrane was held in saline before use. In the gastric media

+90-507 840 65 04
info@vitanaturtr.com

at 0.25, 0.5, 0.75, 1, 2 hours, 500 µl samples were taken and quantified by HPLC. The system was completed with the same media and amount in each sample collection at 37±0.5 ˚C. Three parallel release studies were conducted for each formulation [2].

1.2.1. Kinetic evaluation of *in vitro* drug release data

A variety of mathematical models were used to analyze data from *in vitro* drug release experiments in order to better understand the probable release mechanism of CAB. The appropriate drug release kinetic model was determined using a computer program developed [3]. The best-fit model was chosen based on the correlation coefficients of formulations with the greatest regression values (r^2). Zero order. first order. Higuchi. and Hixson Crowell kinetic models were used to study the behavior of the release mechanism. In addition. for kinetic analysis. the Korsmeyer–Peppas equation was employed [4–6]. The following mathematical methods were used to investigate the release kinetics of the microemulsion formulations:

Equation 1.

Zero-order model: $Q_t = Q_0 + k_0 t$

Equation 2.

First-order model: $Q_t = Q_0 e^{-kt}$

Equation 3.

Higuchi's model: $Q_t = k_H t^{1/2}$

+90-507 840 65 04
info@vitanaturtr.com

Equation 4.

Hixson-Crowell model: $Q_0^{1/3} - Q_t^{1/3} = k_{HC}t$

Equation 5.

Korsmeyer-Peppas model: $f_t = k_m t^n$

Where f_t represents the fraction of drug dissolved in time t. The apparent constants of dissolution rate for the first-order, zero-order, Higuchi model, Korsmeyer–Peppas model, and Hixson–Crowell models are k_f. k_0. k_H. k_m. and k_{HC}. respectively. Q_0 is the starting quantity of drug. and Q_t is the cumulative amount of drug release at time t in the Hixson–Crowell. zero order. first order. and Higuchi's models. In the instance of Korsmeyer–Peppas. "n" represents the release exponent [6].

1.3. Perfusion solution for SPIP Studies

For SPIP tests, perfusion solution (Golytely solution) was made using 5 mM NaCl, 10 mM KCl, 40 mM Na_2SO_4, 20 mM $NaHCO_3$, and 80 mM mannitol. The buffer's pH was adjusted to 7.4 with orthophosphoric acid or a KOH solution. A 0.45 µm membrane filter was used to filter the newly prepared perfusion medium [7]. Purified water (Milli-Q) was added to each component in order to completely dissolve it. The concentration of each drug or marker used in the perfusion experiments was determined by dividing the maximum recommended dose by 250 mL. To accurately represent the highest medication concentration in the gut, this volume should be consumed. [7-9].

+90-507 840 65 04
info@vitanaturtr.com

1.3.1. In-situ SPIP assays and surgical procedure

The Committee for the Use and Care of Animals at Anadolu University authorized all protocols used to conduct animal studies (Protocol No. 2025/30). All in-situ intestinal perfusion investigations employed female Sprague Dawley rats weighing 200–250 g. The rats were given free access to tap water and fasted for around 12 hours the night before each trial.

According to previously reported investigations and published publications, the experimental process for the in-situ SPIP studies was carried out [7,10]. An intraperitoneal injection of a ketamine-xylazine mixture (90–10 mg/kg, respectively) was used to anesthetize the rats. Every animal that is put on a heated surface that is kept at 37±0.5°C. A midline (3–4 cm) incision was made in the belly to expose the small intestine. The flexible PVC tubing (inlet tubing, internal diameter (id) 0.76 mm; outlet tubing, id 1.70 mm) was carefully cannulated into the jejunal segment (10 cm), and the tubings were then connected to the perfusion system. Care was taken, and exposed segments were kept wet with 37°C saline solution, in order to retain an intact blood supply to the segment. Perfusion medium was incubated at 37±0.5°C in a water bath. The surgical site was then wrapped with parafilm to prevent fluid from exposing segment surfaces from evaporating. The peristaltic pump (Minipuls-3, Gilson, France) was used to pump the blank perfusion solution through the gut at a flow rate of 0.5 mL/min for about 20 min. in order to clear out any remaining debris. The cannulated

+90-507 840 65 04
info@vitanaturtr.com

intestinal segment was cleaned before the perfusion solution containing the drugs/markers was administered for 60 minutes at a flow rate of 0.2 mL/min. In tubes, samples were taken from the distal region of the jejunum at intervals of 10, 20, 30, 40, 50, and 60 minutes.

After collection, samples were immediately frozen at -20°C for high performance liquid chromatography analysis (HPLC). According to standards for euthanasia in experimental animals, animals were cervical dislocated to end each experiment. Following each experiment, the intestinal segment's length was measured.

+90-507 840 65 04
info@vitanaturtr.com

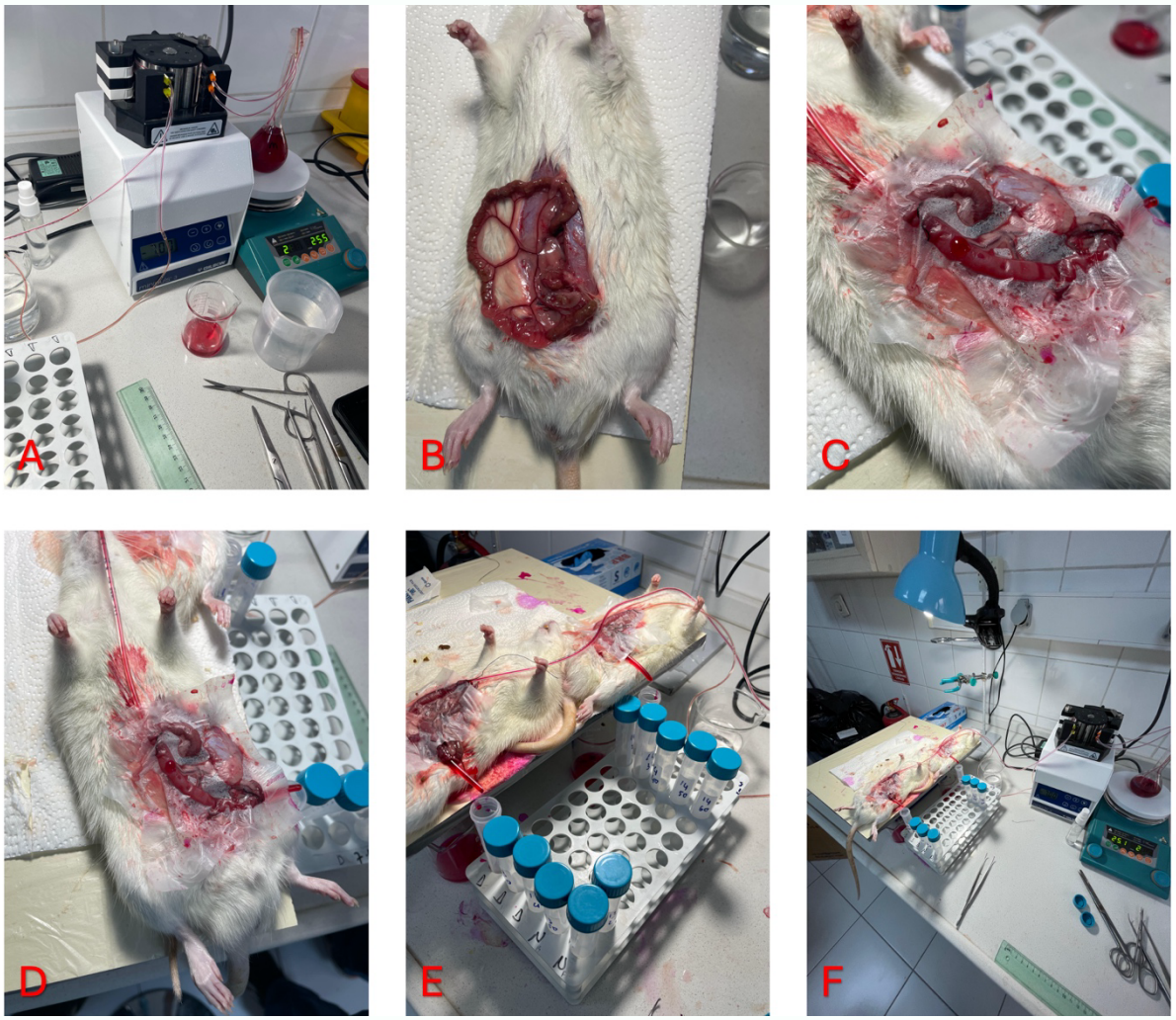

Figure 1. Schematic representation of the experimental setup: (A) peristaltic pump and Golytely solution containing the dissolved active compound; (B) illustration of the ileum; (C) and (D) optimization of the Golytely solution flow; (E) sample collection; and (F) overall view of the experimental setup.

+90-507 840 65 04
info@vitanaturtr.com

1.3.2. Determination of Effective Intestinal Permeability (P_{eff}) Fraction Absorbed in Humans

In order to calculate effective permeability values (P_{eff}) of the drug, the measured C_{out}/C_{in} ratio was corrected for water transport using Equation 6 [11].

Equation 6.

$$\left[\frac{C_{out}}{C_{in}}\right]' = \left[\left(\frac{C_{out}}{C_{in}}\right) \cdot \left(\frac{C_{in\ Phenol\ Red}}{C_{out\ Phenol\ Red}}\right)\right]$$

where $C_{in\ Phenol\ Red}$ is the inlet PR concentration, and $C_{out\ Phenol\ Red}$ is the outlet PR concentration.

Using the "plug flow" model shown in Equation 7, the effective permeability (Peff) values of the medication across the rat gut wall were computed [14].

Equation 7.

$$P_{eff} = \frac{-Q \ln\left[\frac{C_{out}}{C_{in}}\right]'}{2\pi r l}$$

$\left[\frac{C_{out}}{C_{in}}\right]$ is the adjusted drug concentration ratio of outflow to inlet concentration, and Q is the flow rate of the perfusion solution (mL/sec) (Equation 2). For the jejunum, the radius of the perfused intestinal segment is r = 0.2 cm, and the length is l (cm) [8,12,13].

+90-507 840 65 04
info@vitanaturtr.com

Net water flux (NWF) values were calculated based on inlet ($C_{in\ Phenol\ Red}$), outlet ($C_{out\ Phenol\ Red}$) concentrations of PR and (Q_{in}) the inlet perfusate flux using the following Equation 8:

Equation 8.

$$NWF = \frac{\left[1-\left(\frac{C_{out\ Phenol\ Red}}{C_{in\ Phenol\ Red}}\right)\right].Q_{in}}{l}$$

A negative net water flux indicates loss of fluid from the mucosal side (lumen) to the serosal side (blood). A positive net water flux indicates secretion of fluid into the segment [14].

The effective permeability values for humans ($P_{eff\ humans}$) were calculated by using $P_{eff\ rats}$ values obtained from *in-situ* rat SPIP studies, according to the Equation 9 proposed by Fagerholm et al. [15].

Equation 9.

$$P_{eff\ humans} = 3.6P_{eff\ rats} + 0.03x10^{-4}$$

where $P_{eff\ humans}$ = effective permeability predicted for humans, $P_{eff\ rats}$ = effective permeability obtained in rats using SPIP method. The fraction absorbed (F_a) in humans can be calculated for each substance using the Equation 10 presented by Sugano et al.

+90-507 840 65 04
info@vitanaturtr.com

Equation 10.

$$F_a = 1 - e^{-3845.P_{eff\ rats}}$$

Where F_a = fraction absorbed predicted for humans $P_{eff\ rats}$ = effective permeability obtained in rats by SPIP technique.

1.4. Statistical Analysis

The means and standard deviations of all outcomes were reported (SD). The two-tailed non-parametric Mann-Whitney U test was employed to compare the two experimental groups and find any differences. A p value of less than 0.05 was regarded as significant.

2. RESULTS and DISCUSSION

2.1. *In vitro* Release Studies and Kinetic Modelling

The in vitro drug release study was performed for 2 hours in a simulated gastric fluid. Aliquots were withdrawn at predetermined time points of 15, 30, 45, 60, and 120 minutes. Figure 2 illustrates the cumulative percentage drug release profile. The results demonstrate that CAB remained stable under gastric pH conditions and exhibited a rapid release behavior, with approximately 80% of the drug released within the first 15 minutes. This rapid release is attributed to the high aqueous solubility of CAB. Furthermore, more than 95% of the drug was released within 1 hour, indicating complete and efficient dissolution under gastric conditions.

+90-507 840 65 04
info@vitanaturtr.com

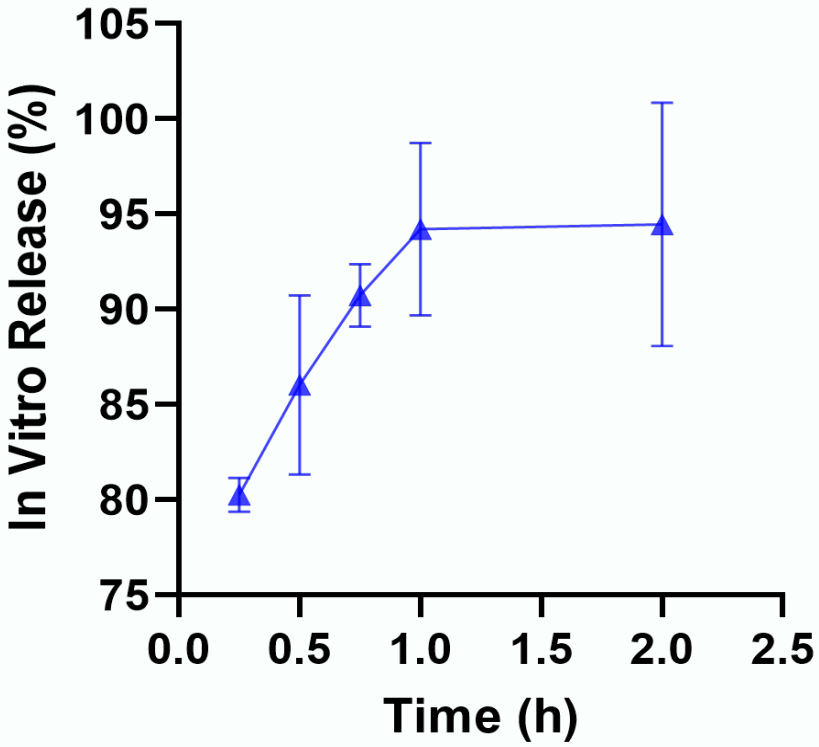

Figure 2. *In vitro* drug release study

The in-vitro release profile of calcium butyrate solution exhibited an initial burst release followed by a diffusion-controlled sustained phase, reaching a plateau at later time points. This release behavior is characteristic of hydrophilic low-molecular-weight compounds evaluated using the dialysis membrane method and suggests Fickian diffusion as the predominant release mechanism.

Cojocaru et al. claim that in order to comprehend the release characteristics, the drug release data should be matched with an appropriate mathematical model. In fact, as the r^2 grows with the number of included parameters, the modified coefficient

+90-507 840 65 04
info@vitanaturtr.com

of determination should be used when comparing models with numerous parameters [16]. Zero-order, first-order, Hixson-Crowell, Higuchi, and Korsmeyer-Peppas models were employed to characterize the kinetics of drug release from the test microemulsions. For each example, the data were converted before being subjected to linear regression analysis. The Hixson-Crowell model can generally be used to examine drug formulations with a range of particle surface area and diameter. The zero-order law can be used to find drug delivery methods where the drug dissolves slowly independent of the initial drug concentration and where the medication does not gradually deteriorate. The first-order law, on the other hand, works better in systems where the initial drug concentration affects drug release. Finally, the release brought on by drug diffusion from the matrix via pore generation is consistent with Higuchi's hypothesis [17].

The r^2 calculation was used to compare the adequacy of each model for describing the drug release kinetics. Table 1 shows the results of fitting the in vitro release data into several kinetic models. The Higuchi model is the most suitable model for formulation. In the Higuchi model,

it is emphasized that the active substance of the drug is released from the matrix structure in a diffusion-controlled manner. The Korsmeyer-Peppas model was used again in the *in vitro* CAB release behavior analysis of these formulations to determine release mechanisms: Fickian (non-steady) diffusional release when $n \leq 0.5$, case-II

+90-507 840 65 04
info@vitanaturtr.com

transport (zero-order) release when n ≥ 1, and non-Fickian, "anomalous" release when n is in between 0.5 and 1 [6,18]. As a result, CAB showed Fickian diffusional release processes since "n" values were 0.577 in gastric medium.

Table 1. Mathematical modeling of in vitro release studies

Kinetic model	r^2	n	k
Zero Order	0.652	7.197	82.660
First Order	0.641	0.036	1.917
Hixon Crowell	0.645	0.121	4.356
Higuchi	0.942	11.112	73.906
Korsmeyer-Peppas	0.924	0.577	1.586

2.2. In-Situ Intestinal Rat Permeability Studies

The cannulation procedures of the intestinal segment were carefully performed to maintain the physiological blood flow of the intestinal segment, the physiological positions of the nerve ligaments, and to ensure normal physiological conditions, and the perfusion flow was set to 0.2 mL / min.

The intestinal membrane integrity was measured using PR, a zero-permeability marker. This marker is widely used in different models of permeability studies [19].

+90-507 840 65 04
info@vitanaturtr.com

Net water flux (NWF) values indicated loss of fluid from the mucosal side (lumen) to the serosal side (blood) in pure CAB group (30±16 mL/h/cm), Water secretion of fluid into the segment was observed. Due to the fact that the absorptive clearance values for chemicals determined from in situ perfusion tests are dependent on loss from the intestinal lumen, Yang et al. believe that NWF must be utilized to modify the concentration of the effluent. Although NWF may play a role in determining absorptive clearance, for drugs with low permeability, the clearance can be approximated using a non-linear equation that approaches a linear connection even if NWF does play a role [20].

Table 2. The net water flux (NWF) in each group (n = 6)

Time (min.)	CAB
10	39±26
20	43±51
30	28±30
40	34±66
50	13±32
60	23±29
Mean±SD	30±16

+90-507 840 65 04
info@vitanaturtr.com

2.3. Permeability of CAB

In all the groups, MTP was administered as a marker to ensure that the experiment was done properly, and PR was utilized as a non-absorbable marker. It is simultaneously perfused with MTP to assess CAB permeability. According to the findings (Table 3), permeability (P_{eff}) was 0.506±0.118 x10^{-4}cm/s for MTP and 1.643±0.439 x10^{-4} cm/s for CAB in rats.

Table 3. Permeability of CABs (n = 6).

Drug	P_{eff} (Human) $(x10^{-4}, cm/s)$	P_{eff} (Rat) $(x10^{-4}, cm/s)$	k_a $(x10^{-3}, 1/s)$	ER
MTP	1.835±0.423	0.506±0.118	14.759±1.858	-
CAB	5.94±1.58	1.643±0.439	19.786±2.887	3.25

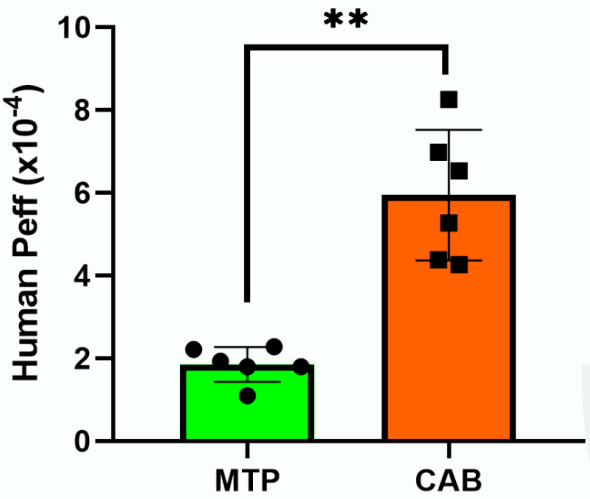

Figure 3. The permeability coefficients (Peff, cm/sec) of CAB calculated from perfusion of rat ileum (mean SD, n=6). **p<0.05, MTP vs CAB Solution

+90-507 840 65 04
info@vitanaturtr.com

Calcium butyrate exhibits significantly higher permeability across the intestinal epithelium compared to metoprolol. This difference arises from fundamental distinctions between the two compounds in terms of their physicochemical properties, ionization behavior, and interactions with transporter proteins in the intestinal epithelium. Primarily, butyrate belongs to the class of short-chain fatty acids (SCFAs) and serves as a major energy substrate for intestinal epithelial cells, particularly colonocytes. The uptake of SCFAs by the epithelium is mediated by transporter proteins such as monocarboxylate transporters (MCTs) and sodium-coupled monocarboxylate transporter 1 (SMCT1). These transporters enable active and facilitated transport of butyrate into enterocytes, thereby markedly enhancing its permeability across the intestinal epithelium [21,22].

The high membrane permeability of butyrate is also attributable to its small molecular size and partial lipophilicity. As a four-carbon short-chain fatty acid, butyrate exhibits a physicochemical profile that is favorable for both paracellular and transcellular transport. In addition, butyrate has a pKa of approximately 4.8, and within the pH range of the small intestine (6.0–7.5), a substantial fraction of the molecule exists in the protonated (non-ionized) form. This non-ionized form can diffuse more readily across lipophilic biological membranes, thereby further contributing to its high permeability [23].

+90-507 840 65 04
info@vitanaturtr.com

In contrast, metoprolol possesses a larger and more complex aromatic structure, and its absorption in the small intestine relies entirely on passive diffusion. Metoprolol has a pKa of approximately 9.7 and is therefore predominantly ionized at physiological small intestinal pH; this significantly retards its passage across lipophilic biological membranes. Moreover, as no specific enterocyte transporter system has been identified for metoprolol, its intestinal permeability is markedly lower than that of butyrate.

In conclusion, the higher permeability of calcium butyrate across the small intestinal epithelium compared with metoprolol can be attributed to its uptake via specific transporters, lower molecular weight, higher proportion of the non-ionized fraction under intestinal pH conditions, and its intrinsic physiological role in enterocyte metabolism.

+90-507 840 65 04
info@vitanaturtr.com

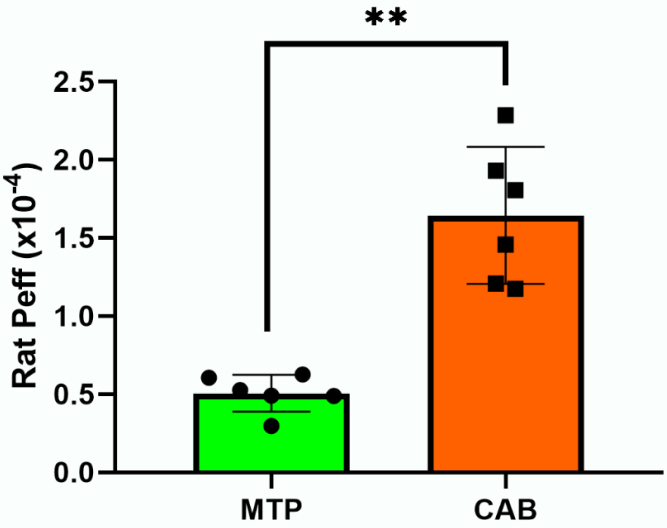

Figure 4. The permeability coefficients (Peff, cm/sec) of CAB obtained from perfusion of rat ileum (mean SD, n=6). **p<0.05, MTP vs CAB Solution

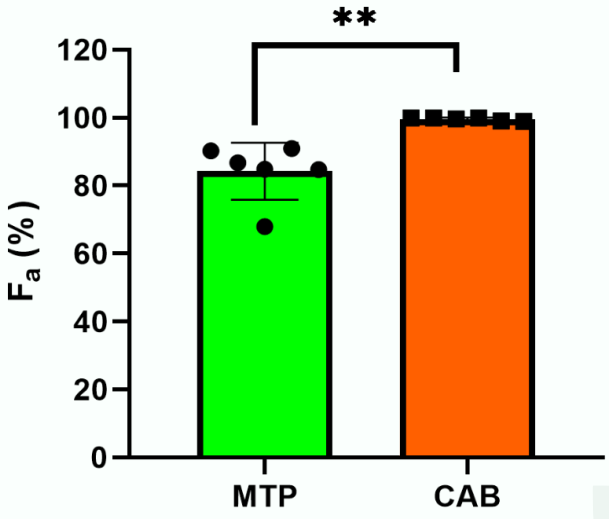

Figure 5. F_a (%) values. **p<0.05, MTP vs CAB

In addition, as seen in Figure 5, fractional absorption of CAB was significantly increased compared to MTP.

+90-507 840 65 04
info@vitanaturtr.com

3. CONCLUSION

The present study demonstrates that calcium butyrate exhibits a characteristic in vitro release profile consisting of an initial burst followed by a diffusion-controlled sustained release phase, which is typical of hydrophilic, low–molecular weight compounds evaluated using the dialysis membrane method. Kinetic modeling revealed that the Higuchi model provided the best fit for the release data, indicating that diffusion from the matrix is the predominant release mechanism. This finding was further supported by the Korsmeyer-Peppas analysis, where the *n* value obtained in gastric medium was consistent with a Fickian diffusion-controlled release process. In situ intestinal perfusion studies confirmed that the experimental setup preserved physiological conditions and membrane integrity, as evidenced by the use of phenol red as a non-permeable marker. Net water flux analysis indicated fluid secretion into the intestinal lumen in the calcium butyrate group, highlighting the importance of correcting effluent concentrations to accurately determine absorptive clearance. Importantly, calcium butyrate demonstrated significantly higher intestinal permeability than metoprolol. This enhanced permeability can be attributed to several complementary factors, including its uptake via specific monocarboxylate transporters (MCTs and SMCT1), its low molecular weight, and its favorable ionization profile, with a substantial non-ionized fraction at intestinal pH. Additionally, the small size and partial lipophilicity of butyrate facilitate both

+90-507 840 65 04
info@vitanaturtr.com

paracellular and transcellular transport, while its physiological role as an energy substrate for intestinal epithelial cells further supports efficient absorption. In contrast, metoprolol, which lacks a specific intestinal transporter and remains predominantly ionized under physiological conditions, exhibits comparatively limited permeability and relies solely on passive diffusion.

Overall, these findings indicate that calcium butyrate combines diffusion-controlled release behavior with intrinsically high intestinal permeability, underscoring its favorable biopharmaceutical properties and supporting its potential for effective intestinal delivery.

+90-507 840 65 04
info@vitanaturtr.com

REFERENCES

1. Özcan S, Çağlar EŞ, Kaynak MS, Üstündağ Okur N. A Newly Developed and Fully Validated HPLC Method for Simultenous Determination of in-situ Single Pass Intestinal Permeability of Domperidone, Metoprolol Tartarate and Phenol Red. *Journal of Research in Pharmacy*. 2023;27(3):967-979. doi:10.29228/jrp.392

2. Nguyen TX, Huang L, Liu L, Elamin Abdalla AM, Gauthier M, Yang G. Chitosan-coated nano-liposomes for the oral delivery of berberine hydrochloride. *J Mater Chem B*. 2014;2(41):7149-7159. doi:10.1039/C4TB00876F

3. Ege MA, Karasulu HY, Karasulu E, Ertan G. A computer program designed for in vitro dissolution kinetics in vitro in vivo kinetic correlations and routine application. In: *4th Central European Symposium on Pharmaceutical Technology*. 2001:127-128.

4. Peppas NA. Analysis of Fickian and non-Fickian drug release from polymers. *Pharm Acta Helv*. 1985;60(4):110-111.

5. Korsmeyer RW, Lustig SR, Peppas NA. Solute and penetrant diffusion in swellable polymers. I. Mathematical modeling. *J Polym Sci B Polym Phys*. 1986;24(2):395-408. doi:10.1002/polb.1986.090240214

6. Ay Şenyiğit Z, Coşkunmeriç N, Çağlar EŞ, et al. Chitosan-bovine serum albumin-Carbopol 940 nanogels for mupirocin dermal delivery: ex-vivo permeation and evaluation of cellular binding capacity via radiolabeling. *Pharm Dev Technol*. 2021;26(8):852-866. doi:10.1080/10837450.2021.1948570

7. Kaynak MS, Buyuktuncel E, Caglar H, Sahin S. Determination of regional intestinal permeability of diclofenac and metoprolol using a newly-developed and validated high performance liquid chromatographic method. *Tropical Journal of Pharmaceutical Research*. 2015;14(1):163-170. doi:10.4314/tjpr.v14i1.23

8. Mancia G, Fagard R, Narkiewicz K, et al. ESH/ESC Guidelines for the management of arterial hypertension: The task force for the management ofarterial hypertension of the european society ofhypertension (esh) and of the european society of cardiology (esc). *J Hypertens*. 2013;31(7):1281-1357. doi:10.1097/01.hjh.0000431740.32696.cc

9. Das S, Chaudhury A. Recent advances in lipid nanoparticle formulations with solid matrix for oral drug delivery. *AAPS PharmSciTech.Springer*. 2011;12(1):62-76. doi:10.1208/s12249-010-9563-0

10. Nagare N, Damre A, Singh KS, et al. Determination of site of absorption of propranolol in rat gut using in situ single-pass intestinal perfusion. *Indian J Pharm Sci*. 2010;72(5):625-629. doi:10.4103/0250-474X.78533

11. Idkaidek NM, Jilani JA, Mansi IA. Evaluation of hydroxyethyldiclofenac intestinal absorption in rats. *Saudi Pharmaceutical Journal*. 2005;13(4):158-163.

12. Zhang Z, Gao F, Bu H, Xiao J, Li Y. Solid lipid nanoparticles loading candesartan cilexetil enhance oral bioavailability: In vitro characteristics and absorption mechanism in rats. *Nanomedicine*. 2012;8(5):740-747. doi:10.1016/j.nano.2011.08.016

13. Li HL, Zhao X Bin, Ma YK, Zhai GX, Li LB, Lou HX. Enhancement of gastrointestinal absorption of quercetin by solid lipid nanoparticles. *Journal of Controlled Release*. 2009;133(3):238-244. doi:10.1016/j.jconrel.2008.10.002

+90-507 840 65 04
info@vitanaturtr.com

14. Kheradmandnia S, Vasheghani-Farahani E, Nosrati M, Atyabi F. Preparation and characterization of ketoprofen-loaded solid lipid nanoparticles made from beeswax and carnauba wax. *Nanomedicine*. 2010;6(6):753-759. doi:10.1016/j.nano.2010.06.003

15. Fagerholm U, Johansson M, Lennernäs H. Comparison between permeability coefficients in rat and human jejunum. *Pharm Res*. 1996;13(9):1336-1342. doi:10.1023/A:1016065715308

16. Cojocaru V, Ranetti AE, Hinescu LG, et al. Formulation and evaluation of in vitro release kinetics of na3cadtpa decorporation agent embedded in microemulsion-based gel formulation for topical delivery. *Farmacia*. 2015;63(5):656-664.

17. Gouda R, Himankar B, Qing Z. Application of mathematical models in drug release kinetics of carbidopa and levodopa ER tablets. *J Dev Drugs*. 2017;6(2):1-8.

18. Lee J, Lee Y, Kim J, Yoon M, Young WC. Formulation of microemulsion systems for transdermal delivery of aceclofenac. *Arch Pharm Res*. 2005;28(9):1097-1102. doi:10.1007/BF02977408

19. Rathore R, Jain JP, Srivastava A, Jachak SM, Kumar N. Simultaneous determination of hydrazinocurcumin and phenol red in samples from rat intestinal permeability studies: HPLC method development and validation. *Journal of Pharmaceutical and Biomedical Analysis*. 2008;46(2):374-380. doi:10.1016/j.jpba.2007.09.019

20. Yang Z, Gan G, Sawchuk RJ. Correlation between net water flux and absorptive clearance determined from in situ intestinal perfusion studies does not necessarily indicate a solvent drag effect. *Journal of Pharmaceutical Sciences.J Pharm Sci*. 2007;96(3):517-521. doi:10.1002/jps.20763

21. Koh A, De Vadder F, Kovatcheva-Datchary P, Bäckhed F. From dietary fiber to host physiology: Short-chain fatty acids as key bacterial metabolites. *Cell*. 2016;165(6):1332-1345. doi:10.1016/j.cell.2016.05.041

22. Cummings JH, Pomare EW, Branch HWJ, Naylor CPE, MacFarlane GT. Short chain fatty acids in human large intestine, portal, hepatic and venous blood. *Gut*. 1987;28(10):1221-1227. doi:10.1136/GUT.28.10.1221

23. Xiong RG, Zhou DD, Wu SX, et al. Health Benefits and Side Effects of Short-Chain Fatty Acids. *Foods*. 2022;11(18). doi:10.3390/FOODS11182863